1992

An Experimental Study of Efficiency and Noise Reduction

P. Yim
Samsung Electronics Company

C. Sung
Samsung Electronics Company

C. Kim
Samsung Electronics Company

S. Oh J. Kim
Samsung Electronics Company

C. Park
Samsung Electronics Company

See next page for additional authors

Authors
P. Yim, C. Sung, C. Kim, S. Oh J. Kim, C. Park, and M. Huh

AN EXPERIMENTAL STUDY OF EFFICIENCY AND NOISE REDUCTION

Yim Pyong-yong*, Sung Chun-mo*, Kim Chang-guk*
Oh Sang-kyoung**, Kim Jung-rae**, Park Chan-woo**, Huh Man-sun**

*Rotary Compressor Division, **R & D Center

SAMSUNG ELECTRONICS CO. Ltd., SUWON, KOREA

ABSTRACT

In this paper, the design parameters were studied to improve the energy efficiency ratio and noise reduction in case of rotary compressor design.

Experimentally, the relationship between the conditions for improving the performance and the valve characteristics, dynamic characteristics of roller and pressure pulsation of rotary compressor were identified. And the influences of geometric parameters to noise were also studied.

Especially, we obtained some results of the design parameters using specially installed test compressor, and applied them to the real compressor to get high performance and low noise level rotary compressor. As the results, efficiency of rotary compressor improved 4.3% and noise level lowered 2dB(A).

NOMENCLATURES

P_s : Suction pressure
P_d : Discharge pressure
P_r : Reference pressure
L_s : Length of suction pipe
P_o : Magnitude of inducing pressure wave
P_o'' : Magnitude of reflecting pressure wave
ω : Angular velocity of inducing pressure wave
ω' : Contacting angular velocity of pressure wave to resonator
ω'' : Angular velocity of reflecting pressure wave
ω_n : Natural frequency of resonator
λ : Wave length of inducing pressure wave
λ'' : Wave length of reflecting pressure wave
t_o : Half period of inducing pressure wave
t_o' : Contacting time of pressure wave to resonator
t_o'' : Half period of reflecting pressure wave
D_p : Pressure depression ratio
C : Speed of sound
S_b : Cross-section area of resonator neck
l_p : Length of resonator neck
ρ_o : Density of refrigerant
γ : Specific heat ratio
M : Mass of refrigerant in resonator neck
K : Stiffness of refrigerant in resonator volume

INTRODUCTION

For designing of a high efficiency and quiet rotary compressor used in room air conditioner, it requires to study the dynamic characteristics of shaft, roller and valve in pump. Pandeya[1] identified the loss mechanism and Wakabayashi[2] classified the losses during suction and compression processes. Recently, a number of papers studied the optimum dimensions and structures of rotary compressor to improve the efficiency and to reduce the noise level[3], and analyzed roller motion by theoretically and experimentally[4].

To reduce the noise level and to predict the noise sources, many researchers studied the shock wave phenomenon of unsteady one-dimensional flow in cylinder[5], and referred to the mechanism of discharge pressure pulsation and acoustic cavity[6]. And CAE approach is used to predict and visualize the 3D acoustic characteristics to reduce the noise of rotary compressor[7].

In this paper, we study the relationship among the valve characteristics, roller dynamics, pressure pulsation and geometric parameters to reduce the noise and to improve the efficiency of rotary compressor.

PERFORMANCE IMPROVEMENT

Experimental apparatus

A rotary compressor with a stroke volume of 12.2 cc/rev was modified as shown in Fig. 1, to measure the pressures, angular position of shaft and discharge valve behavior. Three piezoelectric pressure transducers (Kistler 601A) were used for measuring the dynamic pressures on the lower bearing as shown in Fig. 2. A strain gauge type pressure transducer was mounted on the suction pipe of accumulator to obtain accurate PV diagram. The rotational angle of shaft and TDC(top dead center) position were detected with eddy current type proximity probe which detects revolution of disk with teeth fixed on the motor rotor. The discharge valve behavior was also measured with a proximity probe mounted on the valve backer. The temperatures of discharged refrigerant gas and oil were measured with thermocouples. Power consumption, refrigerating capacity and actual gas flow rate were measured by a secondary refrigerant calorimeter. All data in this paper are obtained under operating conditions ASHRAE "T" of compressor as shown in Table 1.

Table 1 Operating conditions
(ASHRAE "T")

Condensing Temp.	54.4℃ (130°F)
Evaporating Temp.	7.2℃ (45°F)
Suction Temp.	35.0℃ (95°F)
Sub-cool Temp.	46.1℃ (115°F)
Comp-chamber Temp.	35.0℃ (95°F)
Discharge pressure	21.88 Kgf/cm^2 A
Suction pressure	6.38 Kgf/cm^2 A

Experimental results

A schematic diagram of the suction line and cylinder suction chamber is presented in Fig.3. Fig.4 shows the suction pressure with varying the length of suction pipe. The pulsation of suction pressure increases as the length increases. According to the compressor performance shown in Fig. 5, the compressor efficiency and volumetric efficiency are increased as the suction pipe lengthens.

A measured value of gas pressure in the cylinder, TDC position and valve behavior with varying the discharge port diameter are shown in Fig.6. Discharge passage loss and re-expansion loss are caused by the discharge port dimension. The above-mentioned losses are evaluated using the result of P-V diagram gained by measurement of cylinder pressure. Discharge passage loss and re-expansion loss are shown in Fig. 7, in which the horizontal axis is the discharge port diameter ratio.

The following results are obtained by these experimental analysis. The clearance volume increases as the discharge port diameter increases. An ascending rate of pressure in the compression chamber is lowered in the latter half of compression process, and the opening time of discharge valve is delayed because it is determined by the difference in pressure of both faces. After closing of discharge valve, re-compression phenomenon in compression chamber becomes also small. However, it is found that the discharge port diameter has no great influences on volumetric efficiency, as shown in Fig. 7.

As a result, the discharge passage loss and the indicated power decrease, accordingly total loss of compressor decreases regardless of the increase of re-expansion loss depending upon the suitabel discharge port diameter.

MEASUREMENT OF ROLLER MOTION

Roller motion is measured using radial slots of roller and 4 proximity probes, which sense the slot of roller, installed in lower bearing. The radial slots of roller which have a different depth to identify absolute angular position of roller are filled with epoxy and ground flat. The rotational angle of the shaft is measured using proximity probe as shown in Fig. 1. The roller and probes arrangement used in this test and an example of measured signal are shown in Fig. 8. These signals are processed by the data acquisition system and computer to calculate roller motion.

Fig. 9 shows the average rotational speed of shaft and roller. In case of same suction pressure of compressor, the average roller rotational speed is decreases as the discharge pressure increases. And the variation of angular velocity of roller increases as the rate of roller rotation decreases. Fig. 10 shows the time vs rotation angle of roller for test condition 1 and 4.

NOISE REDUCTION

Compressor noise analysis

Fig. 11 shows measuring points of noise and sound intensity. Tests were performed and it was found that structural vibration of accumulator and cavity resonance of compressor have great effects to noise. Discharged gas through muffler holes is thought as a main cause of cavity resonance. Table 2 shows the test results of 1/3 octave sound intensity measurement.

Table 2 The results of sound intensity

Noise sourse	Frequency (KHz)	Direction
Accumulator	2, 2.5, 3.15	0°
Muffler exit	1.25	45°, 225° (Exit direction)

Resonator

Resonator in Fig. 12 can be modeled as a mass-spring system and reduces pressure pulsation of compressed gas. In this paper, pressure pulsation is regarded as propagation of shock wave[5] and resonator is considered as a depressor of pressure pulsation. Fig. 13 shows schematic process of pressure depression. As shown in Fig. 13, inducing shock wave of magnitude P_o and angular velocity ω is deflected at resonator and becomes a wave of magnitude P_o'' and angular velocity of ω''. Pressure depression ratio, D_p, can be calculated as follows.

$$D_p = \frac{P_o''}{P_o} = \frac{\lambda}{\lambda''} = \frac{t_o'}{2t_o''-t_o} = \frac{\omega'}{2\omega - \omega'} \tag{1}$$

Here, ω' is the solution of following equation.

$$P(\omega') = \frac{\omega'^2}{\omega_n(2\omega - \omega')} \cdot \frac{P_o S_b}{M(\omega_n^2 - \omega'^2)} \sin\frac{\pi\omega_n}{\omega'} + C\pi\left(\frac{1}{\omega'} - \frac{1}{\omega}\right) = 0 \tag{2}$$

where, $M = \rho_o S_b l_p$, $K = \frac{\gamma P S_b^2}{V}$

Table 3 lists dimensions of test and analysis models and Fig. 14 shows the results of analysis. Sample 3 has a better depression ratio than any other samples, and it can be found that as the volume of the resonator becomes larger, depression ratio also becomes smaller. But it also shows that neck length has a optimum value. Fig. 15 is the results of noise test and Fig. 16 shows pressure pulsation inside the cylinder (P_r position) of sample 3 and that of without resonator. As shown in Fig. 17, sample 3 has 3-8dB(A) noise reduction effect in 2-6KHz frequency range. The results of theoretical analysis and that of experimental test have a good agreement.

Table 3 Dimensions of test and analysis models

	w/o reso.	sample 1	sample 2	sample 3
V ratio	–	1	0.24	1.23
l_p ratio	–	1	1.17	0.95

$\gamma = 1.3$, $\rho_o = 71.2 Kg/m^3$, $C = 180 m/sec$, $P = 21.88 Kgf/cm^2 A$

Muffler

In this study, the relation between exit location of discharge muffler and compressor inner cavity resonance is examined. For the test, 5 types of muffler are suggested as shown in Fig. 18. Sample 1 is original muffler with two discharge exits. Sample 2 has no discharge exit and useful results are obtained from the noise test. As shown in Fig. 19, sample 2 has great noise reduction in 1.25KHz range on 90° direction and it can be thought that geometrical shape of valve backer prevent gas from discharging through exit on 270° direction. Though, sample 2 has good noise reduction on all directions, because gas is discharged through clearance between muffler and upper bearing, oil forming happens and it is not recommandable pheonomenon for reliability. In case of sample 3, there is noise reduction in 1.25KHz range but noise in 3.15KHz range becomes higher because of the resonance of rotor bottom cavity. Sample 4 is not recommandable because it is especially noisy on 180° direction. In case of sample 5, by enlarging exit on 270° direction, discharge gas flows more easily to that direction. As a result, noise in 1.25KHz range becomes lower on 90° direction and higher on 270° direction as shown in Fig. 20. So, we can reduce the noise level of 90° direction where is relatively noisy compared with other directions.

Accumulator

From the noise and sound intensity test, structural vibration of accumulator was turned out as a main noise source of 0° direction in 2-3.15KHz frequency range. To diminish noise level, bracket (shown in Fig.11) is lowered to shift vibration frequency of the accumulator to higher frequency.

Fig.21 shows the result. Noise level in 1-2.5KHz frequency range lowered about 4-10 dB(A) and in total 1.88 dB(A).

CONCLUSIONS

1. The discharge passage loss and the indicated power decrease, accordingly total loss of compressor decreases regardless of the increase of re-expansion loss depending upon the suitabel discharge port diameter.
2. In case of same suction pressure of compressor, average angular velocity of roller is decreases but the variation increases as the discharge pressure increases.
3. Pressure pulsation inside the cylinder can be reduced by resonator and as the volume of the resonator becomes larger, depression ratio also becomes smaller. But the neck length has a optimum value.
4. Cavity noise are largely influenced by the exit location and size of discharge muffler.
5. Structural borne noise of accumulator can be reduced by appropriate holding position of accumulator, effectively.

ACKNOWLEDGEMENTS

We would like to thank Mr. Back Mun-ku who is a mechanism designer at R&D center of SAMSUNG ELECTRONICS for his help to sucess this project.

REFERENCES

[1] P. Pandeya et al., "Rolling piston type rotary compressors with special attention to friction and leakage," PCTC 1978, Purdue university

[2] H. Wakabayashi et al., "Analysis of performance in a rotary compressor," PCTC 1982, Purdue university

[3] K. Asami et al., "Improvements of noise and efficiency of rolling piston type refrigeration compressor for household refrigerator and freezer," PCTC 1982, Purdue university

[4] T. Yanagisawa et al., "Motion analysis of rolling piston in rotary compressor," PCTC 1982, Purdue university

[5] S. Kawaguchi et al., "Noise reduction of rolling piston type rotary compressor," PCTC 1986, Purdue university

[6] M. Kakuda et al., "Investigation of pressure pulsation in suction pipe on rotary compressor," PCTC 1988, Purdue university

[7] N. Shige et al., "Prediction & visualization of a three dimensional sound field to reduce the noise of rotary compressors," PCTC 1990, Purdue university

[8] James W. Bush et al., "Identification and reduction of rotary compressor pure tone noise sources using random noise excitation," PCTC 1990, Purdue university

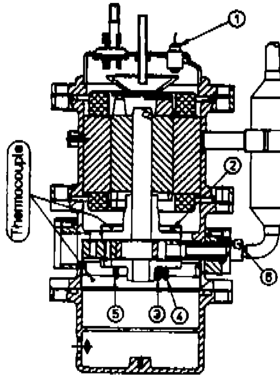

Fig. 1 Test compressor

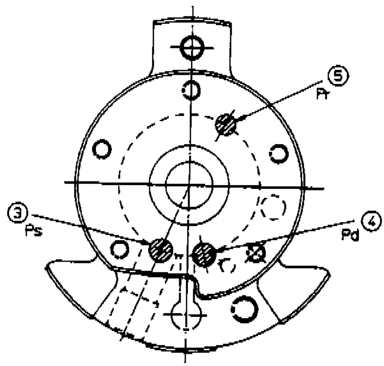

Fig. 2 Pressure transducer mounting

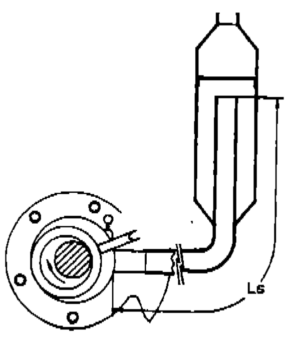

Fig. 3 Cylinder and suction line

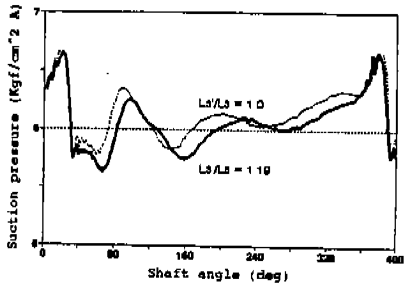

Fig. 4 Influence of suction pipe length to pressure pulsation in suction chamber

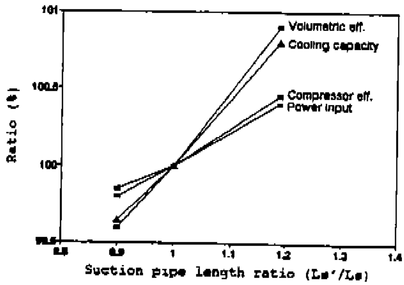

Fig. 5 Suction pipe length effects on compressor performances

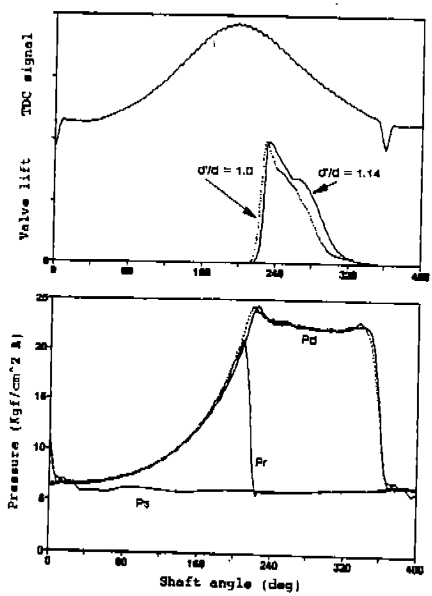

Fig. 6 Influence of discharge port dia. to valve behavior and pressure

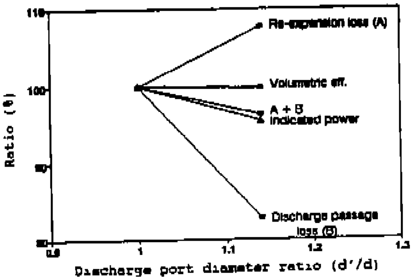

Fig. 7 Discharge port diameter effects on compressor performances

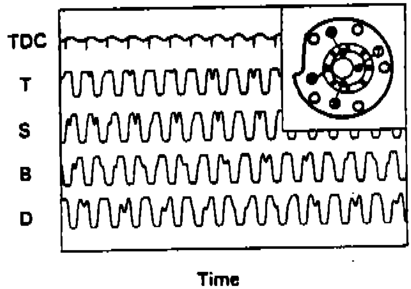

Fig. 8 Probes arrangement and measured signals

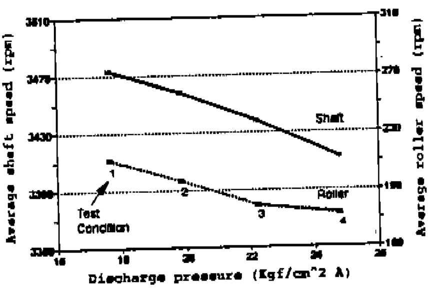

Fig. 9 Average rotational speed of shaft and roller

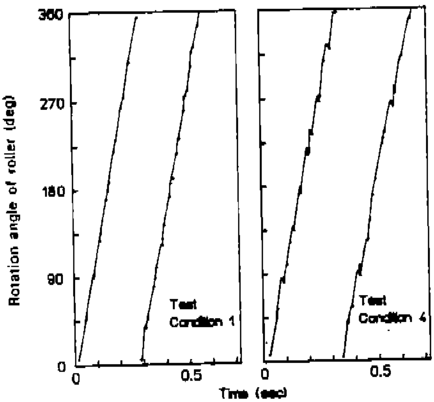

Fig. 10 Rotation angle of roller

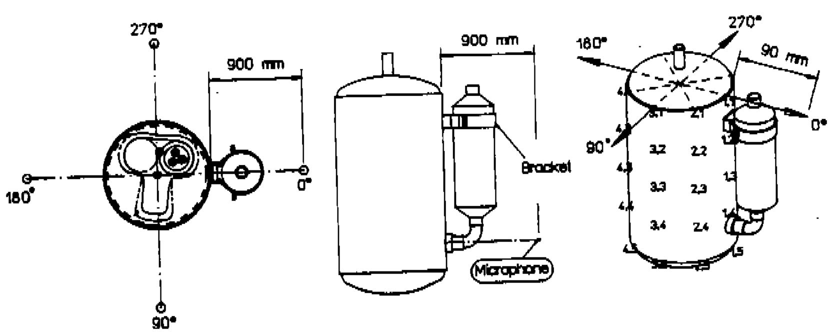

(a) Noise test

(b) Sound intensity test

Fig. 11 Measuring points of noise and sound intensity test

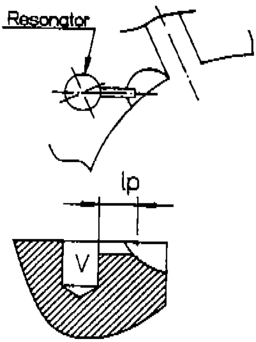

Fig. 12 Resonator

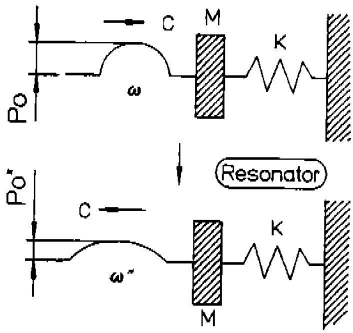

Fig. 13 Pressure depression of resonator

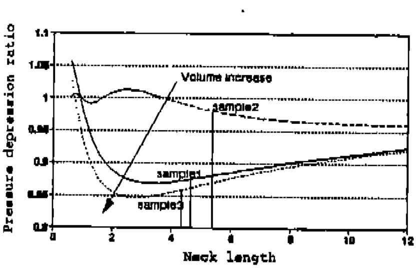

Fig. 14 Pressure depression ratio with varing volume and neck length

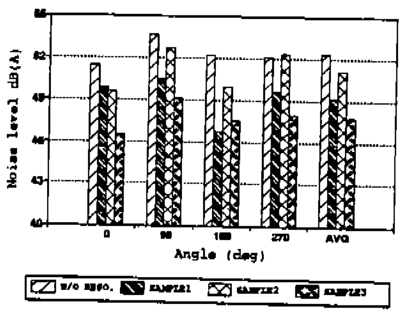

Fig. 15 Result of resonator noise test

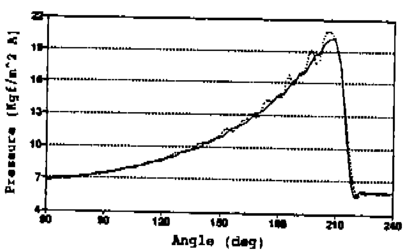

···· W/O Reso. —— Sample 3

Fig. 16 Pressure pulsation at P_r position

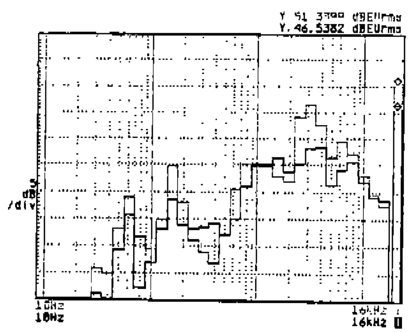

···· W/O Reso. —— Sample 3

Fig. 17 Noise spectra of Resonator test

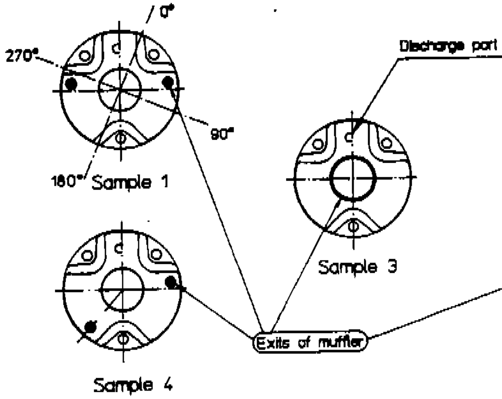

Fig. 18 Exit shape of mufflers for test

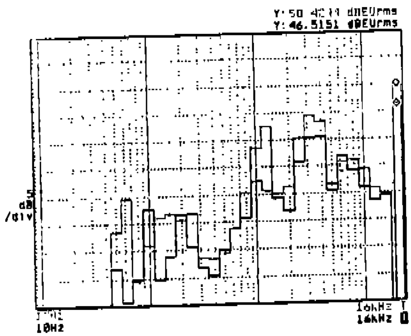

···· Sample 1 —— Sample 2

Fig. 19 Noise spectra of muffler test at 90°

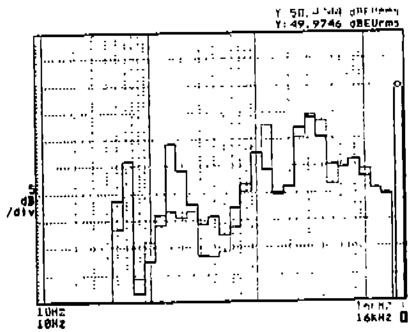

···· Sample 1 —— Sample 5

(a) 90°

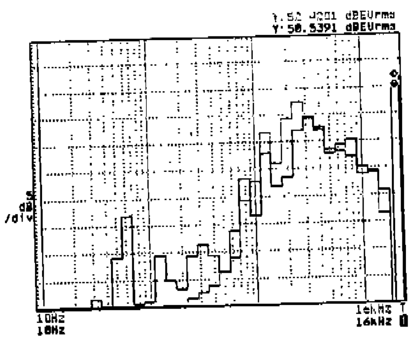

···· Original —— Low bracket

Fig. 21 Noise spectra of accumulator test

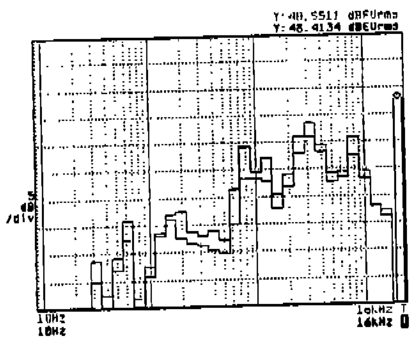

···· Sample 1 —— Sample 5

(b) 270°

Fig. 20 Noise spectra of muffler test